JOURNAL OF SOLID STATE CHEMISTRY 33, 159–167 (1980)

# An Experimental and Theoretical Study of Crystals of Calcium Fluoride Doped with Alkali Metal Cations

P. W. M. JACOBS AND S. H. ONG

*Department of Chemistry, University of Western Ontario, London, Ontario N6A 5B7, Canada*

AND A. V. CHADWICK AND V. M. CARR

*University Chemical Laboratory, University of Kent, Canterbury, Kent, England*

Received May 17, 1979

Experimental measurements of thermal depolarization in crystals of $CaF_2$, grown from the melt containing LiF, NaF, KF, or RbF, reveal a common relaxation (designated $M2$) with an activation energy of 0.51 eV. In addition, the $Li^+$- and $K^+$-doped crystals exhibit a relaxation ($M1$) with an activation energy of 0.34 eV. A similar relaxation has been found in $CaF_2:Rb^+$ by J. Fontanella private communication) and in $CaF_2:Na^+$ by R. D. Shelley and G. R. Miller (*J. Solid State Chem.*, **1**, 218, 1970). Theoretical calculations on $M^+$-doped $CaF_2$ (where $M$ = Li,Na,K,Rb) are in agreement with the hypothesis that the $M2$ relaxation is due to $Na^+$ in all four systems studied and is associated with the jump of a nearest-neighbor (nn) anion vacancy ($F_v^-$) around the substitutional $Na^+$ ion ($Na_s^+$). The assignment of $M1$ is less certain, but it appears to be associated with similar $Li_s^+$–$F_v^-$ dipoles resulting from $Li^+$ impurity present because of the lower volatility of LiF compared to that of KF and RbF. When LiF dissolves in $CaF_2$ the $Li^+$ ion also forms quadrupoles consisting of a cation vacancy and two $Li^+$ interstitials and the reorientation of these quadrupoles has also been studied theoretically.

## Introduction

When a univalent fluoride is incorporated into the alkali earth fluoride, there are several possibilities. It has generally been assumed that doping with NaF leads to $F_v^-$ vacancies. In this case there are eight equivalent nearest-neighbor (nn) positions (Fig. 1a). the next-nearest-neighbor (nnn) site has 24 equivalent positions. This complex has a low symmetry since it has a ⟨311⟩ axis and the study of its properties is therefore very complicated. Alternative possibilities include both univalent $M^+$ and $F^-$ ions entering interstitial sites, or univalent ions replacing cations on normal lattice sites, accompanied by $M^+$ interstitials (Figs. 1b and c). The only extensive examination of this question is that by Franklin (*1*), who calculated the energies of solution of $YF_3$ and NaF in $CaF_2$. These calculations indicate that the lowest energy of solution of NaF occurs with the substitution of $Na^+$ ions on cation sites accompanied by either interstitial $Na^+$ ions or $F^-$ vacancies. However, the preferred mode of solution might change from system to system (e.g., $CaF_2:NaF$ and $BaF_2:KF$) or it might be influenced by the pairing of complementary defects. Therefore, the interpretation of the

0022-4596/80/080159-09$02.00/0

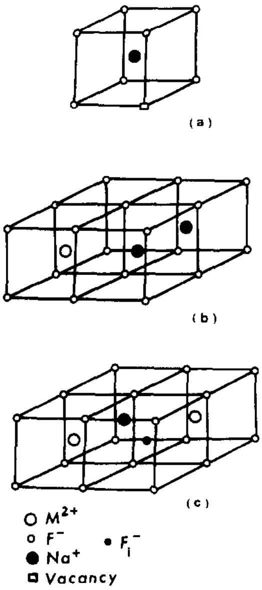

FIG. 1. Three possible configurations for a univalent cation and associated charge-compensating defects in the fluorite structure: (a) a substitutional univalent ion + a fluorine ion vacancy; (b) a substitutional univalent ion + a univalent ion in an interstitial site; (c) univalent and $F^-$ ions in interstitial sites ($F_i^-$ means a fluoride ion at an interstitial site).

properties of $M^+$-doped fluorite crystals is not straightforward since it is not known in general whether the $M^+$ ion will enter substitutionally and/or interstitially.

The purpose of this paper is to try to clarify this problem through a study of a series of alkaline fluorides doped into calcium fluoride crystals. The experimental technique used is that of thermal depolarization (TD). This method was first introduced about a decade ago by Bucci and coworkers (*2, 3*) who coined the term ionic thermocurrents (ITC) to describe the effect. Relaxation effects in the orientation polarization of crystals of alkaline earth fluorides doped with trivalent cations have been successfully carried out by TD measurements (*4–8*). The advantage of the TD technique is its sensitivity and accuracy as compared with that of other relaxation measurements (*3*); also it gives a complete picture of the temperature-dependent relaxations and allows the kinetic parameters for each relaxation to be obtained from a single measurement. The equation governing the depolarization current density (*3*) is

$$j(T) = (P_0/\tau_0) \exp(-E/kT)\exp\{(-1/b\tau_0) \int_{T_0}^{T} \exp(-E/kT')dt'\}, \quad (1)$$

where $b$ is the constant heating rate and $\tau_0$ the reciprocal of the frequency factor. The relaxation time $\tau$ of the dipoles depends on the activation energy for reorientation, $E$, through the Arrhenius equation

$$\tau = \tau_0 \exp(E/kT). \quad (2)$$

$P_0$ is the initial polarization. It depends on the temperature of polarization $T_p$, the time of polarization $t_p$, the polarizing field $\mathcal{E}_p$, the relaxation time $\tau_p$ of the dipoles at $T_p$, the number of dipoles $N_p$ per unit volume, and their dipole moment $p$ through the equation

$$P_0 = \frac{N_p p^2 \mathcal{E}_p}{3kT_p}\left[1 - \exp\left(-\frac{t_p}{\tau_p}\right)\right]. \quad (3)$$

Experimental $j(T)$ curves can be computer fitted (*9*) to Eq. (1) to yield numerical values of $P_0$, $E$, and $\tau_0$. Commonly, one measures the current rather than the current density in which case the experimental parameters are $E$, $\tau_0$, and the total stored charge $Q_0 = P_0A$, where $A$ is the area of the crystal between the electrodes. The TD experiment thus reveals information about the activation parameters involved in the removal of polarization and these should be consistent with any model proposed for the polarization process.

## Experimental

The $CaF_2:Na^+$ crystals were obtained from Atomic Energy of Canada Ltd., Chalk River, with the nominal dopant concentration of 0.1 mole%. The $Li^+$-, $K^+$-, and $Rb^+$-

doped crystals also had the same nominal concentration of 0.1 mole% and were grown at the University of Kent Chemical Laboratory. These crystals were prepared by adding the corresponding fluoride to the $CaF_2$ powder prior to growth. Crystals (10 mm diameter × 50 mm length) were grown from this powder by the Stockbarger technique using graphite crucibles (Ultra Carbon, UF4S grade) and a radiofrequency induction furnace. The growth chamber was flushed continuously with argon (B.O.C.) during the growing procedure. The optimum conditions were found to be a growth rate of 20 mm per hour followed by an anneal for several hours at approximately 1000 K, and finally cooling to room temperature at 4 K per minute.

The procedure used for the TD measurements was the usual one (*3*). The sample was polarized to saturation, in an electric field $\mathscr{E}_p$ ranging from 2000 to 5000 V $cm^{-1}$, at an appropriate temperature $T_p$ such that any dipoles present are sufficiently mobile to become oriented in the field. The polarization cell was then cooled to a low temperature at which the motion of the dipoles is frozen and the electric field removed. On warming at a constant rate (4 K/min) a current pulse is recorded in the temperature range in which the frozen-in polarization disappears as the dipoles randomize. The linear heating rate was achieved by the use of a Stanton Redcroft Model 681 linear temperature programmer and the depolarization current was measured using a vibrating reed electrometer (Cary 401). The noise level of the apparatus was about 5 × $10^{-15}$ A. The TD current and thermocouple readings were continuously monitored by a two-pen Hewlett-Packard chart recorder.

TABLE I

RELAXATION PARAMETERS FOR $CaF_2:M^+$

| Impurity | Peak No. | $T_m$ (K) | $\rho_0$ (sec) | $E$ (eV) |
|---|---|---|---|---|
| $Li^+$ | $M1$ | 121 | $7.18 \times 10^{-13}$ | 0.334 |
| | $M2$ | 163 | $1.97 \times 10^{-14}$ | 0.502 |
| $Na^+$ | $M1$ | 120 | — | 0.38[a] |
| | $M2$ | 167 | $1.69 \times 10^{-14}$ | 0.522 |
| $K^+$ | $M1$ | 122 | $4.16 \times 10^{-13}$ | 0.353 |
| | $M2$ | 168 | $2.94 \times 10^{-14}$ | 0.513 |
| $Rb^+$ | $M1$ | — | — | 0.32[b] |
| | $M2$ | 163 | $1.24 \times 10^{-14}$ | 0.511 |

[a] Shelley and Miller (*12*).

[b] Fontanella (private communication).

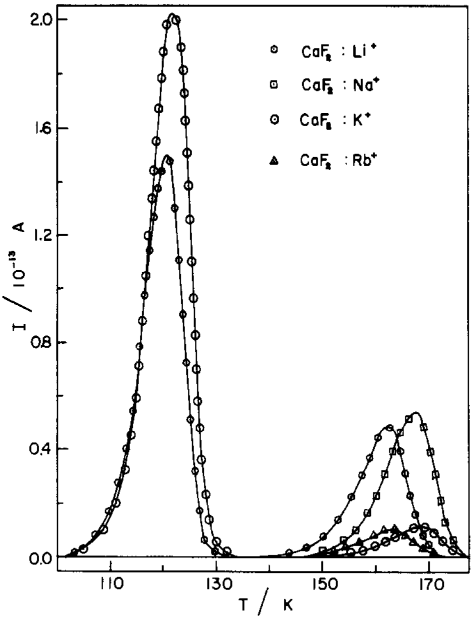

FIG. 2. Thermal depolarization of $CaF_2:M^+$.

## Results

The results of TD measurements on $CaF_2:M^+$ crystals are presented in Table I. The values given are the average results for at least two crystals, more than one run being done on each crystal. Figure 2 shows the whole spectrum for the series of $CaF_2:M^+$ crystals. We call the peak at about 120 K $M1$ and that at 165 K $M2$. The results for $CaF_2$: $Na^+$ have been reported elsewhere (*10*) but are included here to complete the series $Li^+$ through $Rb^+$. From

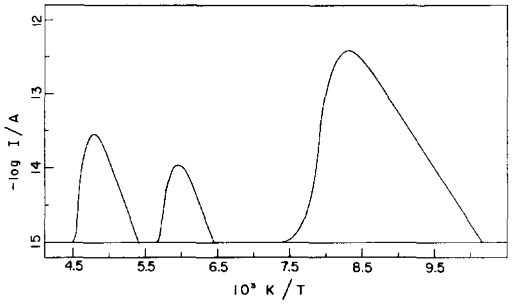

FIG. 3. Thermal depolarization of $CaF_2: K^+$.

Fig. 2 and Table I, we notice that $CaF_2: Li^+$ and $CaF_2: K^+$ behave anomalously in that the main relaxation exhibits a low activation energy. These low activation energies were also found in the recent dielectric measurements of J. Fontanella (private communication), who also used crystals from the same source. The agreement between these measurements and our own is excellent. The ratio of $M1$ to $M2$ is 3 : 1 in $CaF_2: Li^+$ and 20 : 1 in $CaF_2: K^+$. In $CaF_2: K^+$, in addition to $M1$ and $M2$, there is another peak at 209 K with $E = 0.609$ eV, $\tau_0 = 2.10 \times 10^{-13}$ sec (Fig. 3). This third peak is not included in Fig. 2 because only two out of seven samples studied showed this peak.

The results for $CaF_2: Na^+$ are in agreement with those of other workers (*11, 12*). The single relaxation has been attributed to the motion of an nn vacancy around the alkali metal ion substituting for $Ca^{2+}$ on a normal cation site. In comparing the results for series of $CaF_2: M^+$ crystals, we can come to two possible conclusions:

(1) The $M2$ relaxation in $Li^+$, $K^+$, and $Rb^+$ is so close to that of $Na^+$ that it could be ascribed to $Na^+$ in these crystals. If we assign all the $M2$ peaks observed to a $Na^+$ impurity, then the vacancy jump activation energy is 0.33 eV for $Li^+$, 0.52 eV for $Na^+$, and 0.35 eV for $K^+$. It is hard to understand why $E$ should not be a smooth function of ion radius.

(2) If we combine our data with the results of Shelley and Miller (*12*), who found, for $M1$, $E = 0.38$ eV at 120 K in $CaF_2: Na^+$ and those of Fontanella (private communication), also for $M1$, who obtained $E = 0.32$ eV in $CaF_2: Rb^+$, we come to the conclusion that all four systems show two sets of activation energies: one ~0.52 eV and the other ~0.35 eV (see Fig. 2). The 0.52-eV peak is confirmed by dielectric and mechanical relaxation experiments on $CaF_2: Na^+$ reported by Johnson *et al.* (*11*). As pointed out by Lidiard (*13*) the absence of a mechanical relaxation when the applied stress is along ⟨100⟩ confirms that the defect has the trigonal symmetry expected for a nn $M_s^+$–$F_v^-$ complex. The problem then is how to explain the 0.35-eV relaxation. The calculations of Franklin show that the $M_i^+$–$F_i^-$ charge compensation configuration is rather unstable (for $M$ = Na); instead these results favor $M_s^+$–vacancy and $M_s^+$–$M_i^+$ defects. If we assign the 0.52-eV relaxation to the $M_s^+$–$F_v^-$ complex we are left with two problems: why the activation energy is apparently independent of the radius of $M^+$ and what is the origin of the 0.35-eV relaxation. In view of the impasse reached in the interpretation of these experimental results we decided to undertake detailed calculations on the system $CaF_2: M^+$ and these are described in the next section.

## Theoretical Calculations

We use the method originally due to Mott and Littleton (*14*) as formulated in the HADES program written by Norgett (*15*). The method and this program have been tested thoroughly in calculations on alkali halides (*16, 17*) and alkaline earth fluorides (*18*) and have been shown to yield reliable results when satisfactory two-body potentials are available. Here we used the $Ca^{2+}$–$F^-$ and $F^-$–$F^-$ potentials developed by Catlow *et al.* (*18*). For the $K^+$–$K^+$ and $Rb^+$–$Rb^+$ interactions we used the spline potentials of Catlow *et al.* (*19*). The shell parameters were also taken from the work of Catlow *et al.* (*18*, *19*). The remaining Born–Mayer interactions were all calculated by the well-tried electron-gas approximation (*20*, *21*). The potentials used are summarized in the Appendix for ease of reference. The calculations were all performed on the CYBER 73 computer at the University of Western Ontario. The inner region I, comprising the defect and the near-neighbor ions whose relaxations are calculated explicitly, contained at least 100 ions except for the $M_s^+$–$F_v^-$ complex with the $F^-$ ion vacancy in the second neighbor position, for which core restrictions limited the number of ions in region I to 70, due to the low symmetry of the defect.

The calculated energies of solution of $M$F in $CaF_2$ are shown in Table II. The second column shows the energy of solution of $M$F as a substitutional $M^+$ ion and an isolated $F^-$ ion vacancy, while the third column gives the energy of solution if the $M_s^+$ ion and the vacancy are located on nn sites. The absence of a stabilizing $F^-$ ion (Fig. 1a) causes the substitutional ions $Li^+$, $Na^+$, $K^+$ to move away from the vacancy along ⟨111⟩ to the extent shown in column 4. For the small $Li^+$ ion the movement is considerable, amounting to a displacement of 0.50 Å; for $Na^+$ and $K^+$ the displacements are smaller while $Rb^+$ moves toward the vacancy to reduce the overlap with the $F^-$ ion at −0.5, −0.5, −0.5. These movements are just what one would expect from the sizes of the substitutional cations. Column 5 shows the energy of solution of $M$F if the $M^+$ cations are distributed equally on substitutional and (remote) interstitial sites while the sixth column shows the energy of solution if $M$F dissolves to form $M_s^+$–$M_i^+$ nn complexes. For $Na^+$, $K^+$, $Rb^+$ the formation of $M_s^+$–$F_v^-$ nn complexes is favored over that of $M_s^+$–$M_i^+$ nn complexes and to an increasing extent as the radius of $M^+$ increases. The ion positions in column 7 show that the substitutional cations $Na^+$, $K^+$, $Rb^+$ move off slightly in a ⟨100⟩ direction toward the plane of the four $F^-$ ions normal to the $M_s^+$–$M_i^+$ axis and that the interstitial ion also moves in the same direction. For $Li^+$ these ion movements are so exaggerated that the complex assumes the form of a symmetrical ⟨100⟩ dumbbell,

TABLE II

ENERGIES OF SOLUTION (IN eV) OF $M$F IN $CaF_2$[a]

| | | $M_s^+$–$F_v^-$ | | | $M_s^+$–$M_i^+$ | |
|---|---|---|---|---|---|---|
| $M^+$ | $M_s^+ + F_v^+$ | Energy | Displacement | $M_s^+ + M_i^+$ | Energy | Positions of $M^+$ |
| $Li^+$ | 2.63 | 1.63 | 0.107 | 3.46 | 1.29[b] | 0, −0.449,0<br>0, +0.449,0 |
| $Na^+$ | 1.79 | 0.99 | 0.042 | 2.33 | 1.44 | 0, −0.101,0<br>0, +0.912,0 |
| $K^+$ | 1.92 | 1.18 | 0.010 | 3.91 | 2.80 | 0, −0.072,0<br>0, +0.918,0 |
| $Rb^+$ | 2.35 | 1.59 | −0.014 | 5.64 | 4.19 | 0, −0.038,0<br>0, +0.872,0 |

[a] The final state of the $M^+$ ion is indicated in the column headings. The column headed "displacement" shows the value of $a$ for the displacement $-a$, $-a$, $-a$ from the cation substitutional site taken as origin with the vacancy at 0.5, 0.5, 0.5. The column headed "positions" shows the final position of the substitutional and interstitial ions, referred to the substitutional cation site as origin.

[b] Symmetrical ⟨100⟩ dumbbell.

which is the more stable configuration for the incorporation of $Li^+$ impurity in $CaF_2$.

The association energies for the formation of complexes involving $M_s^+$ ions are given in Table III. The complexes all have considerable stability due to the coulomb attraction between the defects. In all four cases the nn $M_s^+$–$F_v^-$ complex is much more stable than the nnn complex as expected because of the enhanced electrostatic attraction in the nn configuration. The $M_s^+$–$M_i^+$ complex would also be formed in preference to the isolated defects, but only in the case of $Li^+$ is this complex favored over $M_s^+$–$F_v^-$ and then it adopts the dumbbell configuration which is almost a double face-centered interstitial with a cation vacancy between the two interstitials.

The activation energies for the jumps of the charge-compensating defect–anion vacancy or $M^+$ interstitial as the case may be–around the substitutional ion are given in Table IV. Within the $M_s^+$–$F_v^-$ complex the vacancy may jump along either the ⟨100⟩ or the ⟨110⟩ directions. The former is favored in all cases, although to a decreasing extent as the radius of $M^+$ increases. The fourth column shows that the activation energy for the orientation of nnn complexes by vacancy jumps along the ⟨100⟩ direction is about 0.27 eV for all four cations (cation size having little effect on the jump of a nnn vacancy) while the fifth column gives the activation energy for the orientation of $M_s^+$–$M_i^+$ complexes. For $Na^+$, $K^+$, $Rb^+$ these are the energies required to take the interstitial $M^+$ ion to the symmetrical saddle point in the cube edge as it jumps along the ⟨110⟩ direction. Data for various possible routes for the reorientation of the $Li^+$ di-interstitial quadrupole are given in Table V. This information suggests that the three-

TABLE III

ASSOCIATION ENERGIES (IN eV) OF COMPLEXES INVOLVING SUBSTITUTIONAL $M^+$ IONS IN $CaF_2$

| | $M_s^+$–$F_v^-$ | | |
|---|---|---|---|
| | nn | nnn | $M_s^+$–$M_i^+$ |
| $Li^+$ | −1.00 | −0.53 | −1.17[a] |
| $Na^+$ | −0.81 | −0.40 | −0.89 |
| $K^+$ | −0.74 | −0.43 | −1.09 |
| $Rb^+$ | −0.76 | −0.45 | −1.45 |

[a] Symmetrical ⟨100⟩ dumbbell (see Table II).

TABLE IV

ACTIVATION ENERGIES (IN eV) FOR THE REORIENTATION OF COMPLEXES INVOLVING $M^+$ IN $CaF_2$[a]

| | | $M_s^+$–$F_v^-$ | | $M_s^+$–$M_i^+$ |
|---|---|---|---|---|
| | nn → nn ⟨100⟩ | nn → nn ⟨100⟩ | nnn → nnn ⟨100⟩ | nn → nn ⟨100⟩ |
| $Li^+$ | 0.40 | 1.75 | 0.29 | b |
| $Na^+$ | 0.50 | 1.78 | 0.28 | 0.91 |
| $K^+$ | 0.74 | 1.64 | 0.26 | 3.02 |
| $Rb^+$ | 0.93 | 1.61 | 0.26 | 3.13 |

[a] The type of complex (nn or nnn) and the direction of motion of the vacancy or interstitial are shown in the column headings.

[b] See Table V.

TABLE V

CALCULATED ACTIVATION ENERGIES (IN eV) FOR THE REORIENTATION OF THE $Li^+$ DI-INTERSTITIAL IN $CaF_2$[a]

| Symmetry axis | Energy of local minimum | Coordinates | Activation energy |
|---|---|---|---|
| ⟨100⟩ | 6.30 | 0,−0.449,0<br>0,+0.449,0 | — |
| ⟨110⟩ | 6.95 | +0.223,−0.223,0<br>−0.768,+0.768,0 | 0.65 |
| ⟨110⟩ | 6.94 | +0.273,−0.273,0<br>−0.273,+0.273,0 | 0.64 |
| ⟨111⟩ | 6.88 | +0.225,−0.225,0<br>−0.225,+0.225,0 | 0.58 |

[a] The coordinates of the two $Li^+$ ions in the initial ⟨100⟩ configuration and in the three saddle points are also given.

dimensional potential energy surface is rather flat, with numerous local minima. As the di-interstitial is not a dipolar defect and will not therefore be detected in a thermal deoplarization experiment, the reorientation mechanism was not explored further.

## Discussion

The results of the calculations described in the previous section illustrate their value in enabling one to discriminate first between various types of complexes that may be formed and second between various types of orientation mechanisms. For $CaF_2:Na^+$ charge compensation by a $F^-$ vacancy is favored over that by a $Na^+$ interstitial by 0.45 eV. Ignoring differences in the entropy of formation, which are likely to be small, this means that the concentration ratio of $M_s^+$–$F_v^-$ complexes to that of $M_s$–$M_i^+$ complexes exceeds 100 at 1000 K and is more than $10^7$ at 300 K. Thus the formation of the former complex in preference to the latter may safely be assumed in $CaF_2:Na^+$, and is overwhelmingly preferred in $CaF_2:K^+$ and $CaF_2:Rb^+$. The complex formed has the vacancy in the nn position (Table III) and orientation of these complexes proceeds by the jump of the vacancy along the ⟨100⟩ direction (Table IV). The calculated activation energy for this process for $CaF_2:Na^+$ is 0.495 eV, in excellent agreement with that for the $M2$ relaxation for all four dopants, viz., 0.502–0.522 eV (Table I). We conclude therefore that the $M2$ relaxation is due to the reorientation of $M_s^+$–$F_v^-$ nn complexes by vacancy jumps along ⟨100⟩ and that for the $Li^+$-, $K^+$-, and $Rb^+$-doped crystals the $M2$ relaxation is due to $Na^+$ impurity. Table VI lists the melting and boiling temperatures of $CaF_2$ and the alkali metal fluorides. We see that the mp of $CaF_2$ is above the bp of RbF and CsF and close to that of KF and we conclude that growing crystals in crucibles open to the ambient atmosphere (Ar) would allow most of the RbF and KF to evaporate while retaining any NaF and LiF impurities. In $CaF_2:K^+$ a TD peak with an activation energy of 0.61 eV was seen in two samples out of seven. This was originally ascribed to an impurity but could be due to a very small amount of $K^+$ retained nonuniformly in the $CaF_2$. The activation energy is rather lower than the calculated value of 0.74 eV for the reorientation of $K_s^+$–$F_v^-$ complexes so the identification, while by no means certain, remains a distinct possibility.

TABLE VI

THE MELTING POINTS AND BOILING POINTS OF SOME FLUORIDE CRYSTALS

| | mp (°C) | bp (°C) |
|---|---|---|
| $CaF_2$ | 1423 | 2500 |
| LiF | 845 | 1676 |
| NaF | 993 | 1695 |
| KF | 858 | 1505 |
| RbF | 795 | 1410 |
| CsF | 682 | 1251 |

The $M1$ peak was seen in $Li^+$- and $K^+$-doped $CaF_2$ but not in $CaF_2:Na^+$ or $CaF:Rb^+$. However, it was observed in $Rb^+$-doped $CaF_2$ by Fontanella (private communication) and a similar relaxation has been recorded in $CaF_2:Na^+$ by Shelley and Miller (*12*). The activation energy for $M1$ (0.34 eV) is reasonably close to that calculated for the reorientation of nnn complexes (0.27 eV) but the nn complex is favored by 0.41 eV in $CaF_2:Na^+$; furthermore it would be rather absurd to ascribe $M1$ to a nnn relaxation of $M_s^+$–$F_v^-$ due to a $Na^+$ impurity in $K^+$- or $Li^+$-doped $CaF_2$ when it was not seen in $CaF_2:Na^+$. The only remaining possibility is that $M1$ is due to a $Li^+$ impurity that remains behind as $Rb^+$ and $K^+$, and $Na^+$ to some extent, distill out of the $CaF_2$. Ignoring entropy differences between the two configurations the concentration ratio of $Li_s^+$–$F_v^-$ complexes to $Li_i^+Ca_v^+Li_i^+$ di-interstitials is calculated to be 0.02 at the anneal temperature of 1000 K; however, this value is quite sensitive to possible entropy differences and to small errors in the calculated energies of solution. A significant fraction of $Li_s^+$–$F_v^-$ complexes is therefore a distinct possibility. The calculated activation energy for the orientation of these complexes (Table IV) is 0.40 eV, which is reasonably close to the experimental value of 0.35 eV for the *M*1 relaxation.

## Appendix

SHELL-MODEL PARAMETERS

| | $Ca^{2+}$ | $F^-$ | $Li^+$ | $Na^+$ | $K^+$ | $Rb^+$ |
|---|---|---|---|---|---|---|
| $Y$ (\|e\|) | 5.24 | −2.38 | 1.267 | 2.216 | 1,076.0 | 204.6 |
| $K$ (eV Å$^{-2}$) | 3,909.0 | 101.20 | 79.85 | 125.20 | 13,430,000.0 | 330,300.0 |

CONSTANTS $A$, $\rho$ IN THE BORN–MAYER FORM $A \exp(-r/\rho)$ FOR THE INTERACTION BETWEEN TWO IONS SEPARATED BY A DISTANCE $r$

| Interaction | $A$ (eV) | $\rho$ (Å) |
|---|---|---|
| $Ca^{2+}$–$F^-$ | 1,272.8 | 0.2997 |
| $Li^+$–$F^-$ | 400.81 | 0.2751 |
| $Na^+$–$F^-$ | 1,798.35 | 0.2526 |
| $K^+$–$F^-$ | 1,821.99 | 0.2831 |
| $Rb^+$–$F^-$ | 2,160.45 | 0.2927 |
| $Ca^{2+}$–$Ca^{2+}$ | 21,701.35 | 0.1949 |
| $Ca^{2+}$–$Li^+$ | 2,182.8 | 0.1934 |
| $Ca^{2+}$–$Na^+$ | 4,519.08 | 0.2164 |
| $Ca^{2+}$–$K^+$ | 4,020.92 | 0.2541 |
| $Ca^{2+}$–$Rb^+$ | 5,368.57 | 0.2587 |
| $Li^+$–$Li^+$ | 1,153.8 | 0.1364 |
| $Na^+$–$Na^+$ | 7,895.4 | 0.1709 |

POTENTIALS OF SPLINE FORM

| | |
|---|---|
| $r < r_b$ | $V(r) = A \exp(-r/\rho)$ |
| $r_b < r < r_m$ | Fifth-order polynomial |
| $r_m < r < r_a$ | Third-order polynomial |
| $r < r_a$ | $V(r) = -C/r^6$ |

INTERACTION CONSTANTS

| Interaction | $A$ (eV) | $\rho$ (Å) | $C$ (ev Å$^6$) | $r_b$ (Å) | $r_m$ (Å) | $r_a$ (Å) |
|---|---|---|---|---|---|---|
| $K^+$–$K^+$ | 3796.9 | 0.2603 | 52.0 | 2.57 | 3.17 | 3.69 |
| $Rb^+$–$Rb^+$ | 6808.1 | 0.2704 | 208.8 | 2.78 | 3.442 | 3.993 |
| $F^-$–$F^-$ | 1127.7 | 0.2753 | 15.83 | 2.0 | 2.726 | 3.031 |

## Acknowledgments

We thank the National Science and Engineering Council of Canada for their support of this work and Dr. J. Fontanella for informing us of the results of his dielectric measurements prior to their publication.

## References

1. A. D. Franklin, *J. Amer. Ceram. Soc.* **50**, 648 (1967).
2. C. Bucci and R. Fieschi, *Phys. Rev. Lett.* **12**, 16 (1964).
3. C. Bucci, R. Fieschi, and G. Guidi, *Phys. Rev.* **148**, 816 (1966).
4. B. S. H. Royce and S. Mascarenhas, *Phys. Rev. Lett.* **24**, 98 (1970).
5. D. R. Stiefbold and R. A. Huggins, *J. Solid State Chem.* **5**, 15 (1972).
6. J. Wagner and S. Mascarenhas, *Phys. Rev. B* **6**, 4867 (1972).
7. E. L. Kitts, Jr., M. Ikeya, and J. H. Crawford, Jr., *Phys. Rev. B* **8**, 5840 (1973).
8. B. P. M. Lenting, J. A. J. Numan, E. J. Bijvank, and H. W. den Hartog, *Phys. Rev. B* **14**, 1811 (1976).
9. A. M. Hor, P. W. M. Jacobs, and K. S. Moodie, *Phys. Status Solidi A* **38**, 293 (1976).
10. S. H. Ong and P. W. M. Jacobs, *Canad. J. Phys.*, in press.
11. H. B. Johnson, N. J. Tolar, G. R. Miller, and I. B. Cutler, *J. Phys. Chem. Solids* **30**, 31 (1969).
12. R. D. Shelley and G. R. Miller, *J. Solid State Chem.* **1**, 218 (1970).
13. A. B. Lidiard, *in* "Crystals with the Fluorite Structure" (W. Hayes, Ed.), Oxford Univ. Press (Clarendon), London (1974).
14. N. F. Mott and M. J. Littleton, *Trans. Faraday Soc.* **34**, 485 (1938).
15. M. J. Norgett, AERE Harwell Report R7650 (1974).
16. C. R. A. Catlow, J. Corish, K. M. Diller, P. W. M. Jacobs, and M. J. Norgett, *J. Phys. Paris* **37**, C7-253 (1976).
17. C. R. A. Catlow, J. Corish, K. M. Diller, P. W. M. Jacobs, and M. J. Norgett, *J. Phys. C* **12**, 451 (1979).
18. C. R. A. Catlow, M. J. Norgett, and T. A. Ross, *J. Phys. C* **10**, 1627 (1977).
19. C. R. A. Catlow, K. M. Diller, and M. J. Norgett, *J. Phys. C* **10**, 1395 (1977).
20. P. T. Wedepohl, *Proc. Phys. Soc.* **92**, 79 (1967).
21. R. G. Gordon and Y. S. Kim, *J. Chem. Phys.* **56**, 3122 (1972).